Lithospheric Structure of the Walvis Ridge From Rayleigh Wave Dispersion

Alan D. Chave

Department of Geology and Geophysics, Woods Hole Oceanographic Institution
Woods Hole, Massachusetts 02543
Department of Earth and Planetary Sciences
Massachusetts Institute of Technology, Cambridge, Massachusetts 02139

Abstract. Rayleigh wave group velocity dispersion has been used to study the lithospheric structure along the Walvis Ridge and for a nearby South Atlantic path. Group velocity is anomalously low in the period range of 15-50 s for both surface wave paths. Results of a formal inversion for the ridge suggest crustal thickening to 12.5 km and anomalously low mantle shear velocity of 4.25-4.35 km/s to depths of 45 km. Lowering the density in this region during inversion does not raise the shear velocity to the oceanic norm. A nearby off-ridge path that covers the Cape Basin and part of the western Walvis Ridge shows no sign of thickened crust. No significant differences from normal oceanic lithosphere exist below 50 km, and no signs of thinning of the lithosphere under the Walvis Ridge are apparent. Other geophysical data rule out a thermal cause for the low mantle shear velocity, and it is likely that unusual mantle composition is responsible.

Introduction

The Walvis Ridge is a long linear feature of high bathymetric relief stretching from the Mid-Atlantic Ridge to the African continental margin in the South Atlantic Ocean (Figure 1). Morphologically, it is divided into two provinces, the continuous blocky ridge section east of 2°E and the irregular seamount-guyot section at the younger western end. Structures like the Walvis Ridge are found throughout the world oceans and are called aseismic ridges, since they do not exhibit the narrow band of seismic activity that characterizes mid-ocean spreading centers. Deep sea drilling evidence indicates that aseismic ridges have undergone subsidence since formation at rates similar to the rate of normal oceanic lithosphere and were formed contemporaneously with the surrounding ocean basins [Detrick et al., 1977]. Many models for the formation of aseismic ridges have been proposed [Dingle and Simpson, 1976], but the 'hot spot' plume hypothesis has received increasing support [Wilson, 1963; Morgan, 1971, 1972; Goslin and Sibuet, 1975; Detrick and Watts, 1979]. While this mode of creation fits well into the kinematic framework of plate tectonics, the impact on the deep structure is less clear.

Detrick and Watts [1979] summarized the available seismic refraction data for aseismic ridges. At least nine lines have been shot, but only one reversed line reaching mantle-like velocities exists, indicating a 16-km-thick oceanic crust overlying a low velocity (V_p = 7.93 km/s) mantle on the Nazca Ridge [Cutler, 1977]. Crustal thickness of at least 25 km has been inferred for the Iceland-Faeroes Ridge [Bott et al., 1971]. Low velocity mantle under a thickened oceanic crust also exists on the Concepcion Bank near the Canary Islands [Weigel et al., 1978]. The refraction lines shot on the Walvis Ridge display layer 2 like velocities of 5.45 km/s at depths of 10 km [Goslin and Sibuet, 1975].

The free air gravity anomaly across aseismic ridges is typically less than 75 mGal, indicating some degree of isostatic compensation. Most investigators have inferred Airy-type compensation by crustal thickening. Goslin and Sibuet [1975] modeled the eastern Walvis Ridge with an Airy crustal thickness of 25 km, but Kogan [1976] preferred a flexural model with a 10 to 15 km crust. Detrick and Watts [1979] used Fourier techniques to show that the ridge could be fit with an Airy model at the blocky eastern end but that a flexural model was best for the western seamount province with a much thinner crust. While gravity data can be used to infer shallow structure, the result depends on initial assumptions and is nonunique. In particular, mantle density changes as large as 0.2 g/cm^3 will result in Airy crustal thickness changes of only a few kilometers.

Owing to the paucity of information on the deep structure of aseismic ridges, the present work was undertaken to determine their lithospheric structure from surface wave dispersion. Surface waves are sensitive to averages of the velocity structure in the vertical direction, with the longer period waves sampling the deeper layers. By measuring the phase or group velocity of Rayleigh waves as a function of period an estimate of the average mantle velocity structure can be made. It will be shown that for the Walvis Ridge a combination of crustal thickening and anomalously low velocity upper mantle material, extending to depths of at least 30-40 km, is required to fit the dispersion data. Crustal thickening is consistent with both seismic refraction and gravity data, while low velocity mantle is suggested for several other supposed hot spot regions [Cutler, 1977; Weigel et al., 1978; Stewart and Keen, 1978].

Data

Because of the narrow, linear shape of aseismic ridges, only limited combinations of source and observation points will produce great circle surface wave paths along the

Paper number 9B0996.
0148-0227/79/009B-0996$01.00

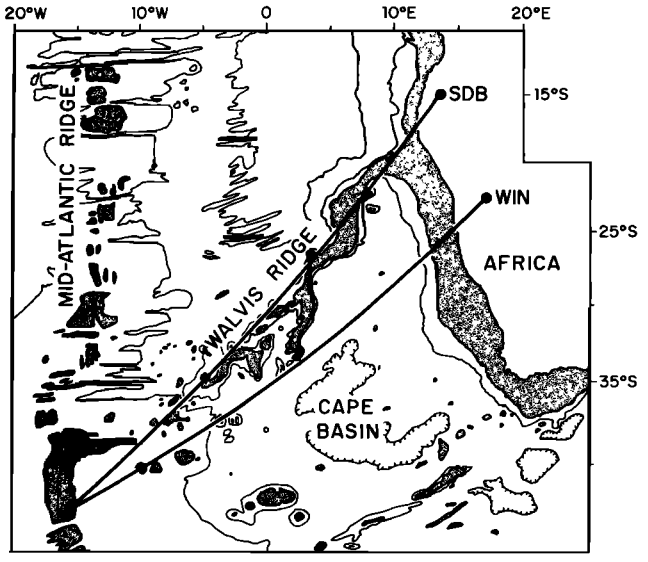

Fig. 1. Bathymetric map showing the great circle paths to stations SDB and WIN. Depths are in thousands of meters, and the stippled area is shallower than 3000 m. Contours are from E. Uchupi and H. Hays [unpublished data, 1978].

strike of the structure. The geographic distribution of World-Wide Standard Seismograph Network (WWSSN) stations severely limits the number of aseismic ridges that can be studied in this way. Although many ridges throughout the world were investigated, only the South Atlantic has the required combination of seismograph station distribution and earthquake sources. In the 15-year period since the advent of WWSSN stations only two suitable events were found. Figure 1 shows their great circle paths to the instruments at Sa da Bandeira, Angola (SDB) and Windhoek, Southwest Africa (WIN). Table 1 summarizes the epicenter information from the International Seismological Center (ISC) Bulletin. Both events are well located owing to the large number of travel time observations with residuals of less than 2 s.

Ideally, one would like to measure both group and phase velocity for these surface wave paths. Group velocity is more sensitive to structural details, particularly above the low velocity zone [Der et al., 1970], but phase velocity produces a more linear forward problem. It is possible to match group velocity dispersion data to widely disparate velocity models, and phase velocity information serves to discriminate between these. There is a trade-off between shallow and deep structure with group velocity due to a zero crossing in the partial derivatives with respect to velocity and density. Computation of group velocity is easy for a single observing station, while computation of phase velocity requires either two stations or assumptions about the source initial phase and one station. A fault plane solution is required to estimate the initial phase using standard earthquake models. The station azimuthal distribution in the South Atlantic is very poor, and no fault plane solutions could be obtained for these events. This study will use only group velocity measurements.

The long period vertical seismograms for each event and station were obtained, digitized at closely spaced (about 0.5 s) intervals, and linearly interpolated to 2-s samples. Figure 2 shows the Airy phases for each event. The wave trains are remarkably clean and free from the beating that would indicate extensive multiple path interference.

Group velocity was determined by the multiple filter technique of Dziewonski et al. [1969]. The group delay time is measured by multiplying the Fourier transformed data by a Gaussian filter centered on the period of interest and searching for the energy peak. The group velocity is the path length, assumed to be least distance or great circle, divided by the group delay time. The great circle distances were calculated using first order corrections for the ellipticity of the earth [Thomas, 1965]. In all cases the instrument response was removed using the equations of Hagiwara [1958] as corrected by Brune [1962], and the instrument resonance and damping parameters from Mitchell and Landisman [1969]. The choice of filter bandwidths is important, since too narrow a filter will ring and produce false peaks, while too wide a filter yields data which are statistically dependent owing to the overlap between adjacent filters. The filters were spaced on equal logarithmic period increments, and the bandwidths were selected by requiring that the uncertainty principle given by Der et al. [1970] be met or exceeded. The computed group velocity for each event was averaged for each path, and the result appears in Table 2 and Figure 3. The high precision of the measurements is reflected in the

TABLE 1. Earthquake Epicenters From ISC Bulletin

	Event 1	Event 2
Date	April 19, 1968	April 19, 1968
Origin Time, UT	0808:21.0 ± 0.23	0904:28.2 ± 0.27
Latitude, °S	42.70 ± 0.054	42.69 ± 0.061
Longitude, °W	16.06 ± 0.056	16.05 ± 0.070
Depth, km	19 ± 0.7	33
Standard Deviation, s	1.12	1.56
M_b	5.0	5.5
Observations	30	50

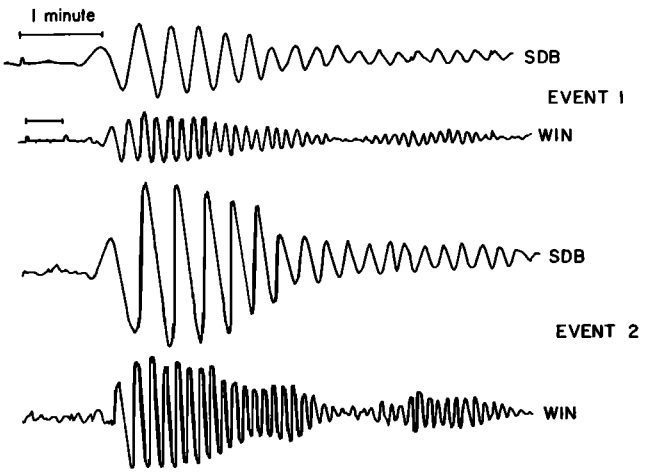

Fig. 2. Airy phases for, from top to bottom, event 1 at SDB and WIN and event 2 at SDB and WIN. The different appearance of the records at the two stations is due to the different speeds of the recording drum.

repeatability to within 0.01 km/s of the two independent determinations for each path.

Error Analysis

An estimate of the probable errors and sources of error was made to see if the difference between the SDB and WIN dispersion was real. Errors in data and analysis techniques can be classified as random or systematic. For digital seismic data, random error includes digitization inaccuracy, quantization noise, and uncertainty in the computation of spectral peaks due to the short data sections that must be used. Digitization errors were checked by multiple analyses on the seismograms and proved to be insignificant. The normal branch of the computed dispersion curves compares favorably to peak and trough measurements for the SDB seismograms. Quantization noise is minimized by using high-amplitude seismic data and a fine digitization increment. The effect of short data sections can be minimized by using wide enough bandpass filters to provide some smoothing. An uncertainty was assigned to each velocity on the basis of the width of the spectral peak and is believed to represent the random error adequately.

Systematic errors will affect only the absolute level of the dispersion curve and cannot explain the shape difference between the South Atlantic and Pacific results in Figure 3. Sources of systematic error include epicenter mislocation and origin time computation, source rise time and finiteness, lithospheric anisotropy, path error, and station timing error. Each of these will be discussed in turn to yield an estimate of the actual uncertainty in the data.

Epicenter mislocation is probably the largest source of systematic error. For these events the path length is near 4200 km, and a radial 10-km error at this range results in a group velocity error of 0.01 km/s. An error of 40-50 km is required to explain the difference between the dispersion seen at SDB and WIN, and mislocation by this amount must be considered unlikely.

Origin time computation errors can occur owing to inhomogeneity in the velocity structure of the earth. The large lateral velocity changes associated with the thermal structure of midocean ridges can lead to origin time errors as large as 1 s [Forsyth and Press, 1971].

Rise time and source finiteness errors arise because no real earthquake is a point source in either time or space. Data on source rise time for small earthquakes are lacking, and it is assumed to be smaller than 1 s. Source finiteness error is of the order of L/V, where L is the fault length and V is the rupture velocity. For small earthquakes (M_b = 5-6) L is near 10 km [Hanks and Thatcher, 1972] and V is in the range of 2-4 km/s [Kanamori, 1970], leading to an uncertainty of about 3 seconds.

Azimuthal anisotropy that is depth and therefore frequency dependent exists in the oceanic lithosphere. Forsyth [1975] reports a

TABLE 2. Group Velocity Data

Period	SDB Group Velocity	Uncertainty	WIN Group Velocity	Uncertainty
13.6	3.220	0.060	3.195	0.080
15.9	3.535	0.030	3.470	0.020
18.5	3.610	0.025	3.635	0.020
21.6	3.710	0.015	3.795	0.025
25.2	3.785	0.025	3.875	0.025
29.4	3.845	0.025	3.935	0.025
34.2	3.885	0.025	3.970	0.020
39.9	3.905	0.025	4.000	0.030
46.5	3.920	0.030	4.005	0.025
54.3	3.925	0.020	4.000	0.020
63.3	3.895	0.040	3.970	0.030
73.8	3.865	0.040	3.950	0.035
86.0	3.850	0.030	3.860	0.020

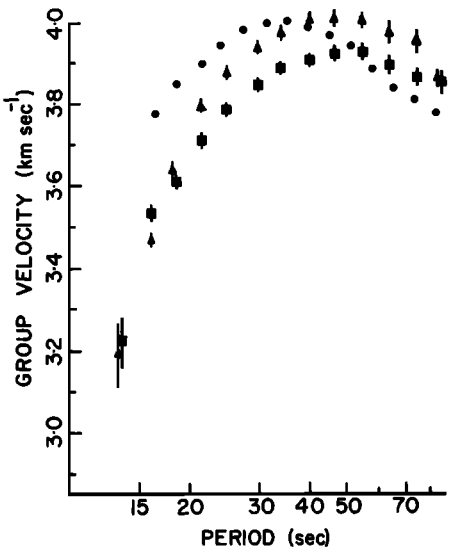

Fig. 3. Group velocity dispersion curves for the two events at SDB (squares) and WIN (triangles) and for the 20 to 50 m.y. pure path result of Forsyth [1973] (circles). Errors are discussed in the text.

maximum anisotropy of 2% in the east Pacific, while Yu and Mitchell [1979] found no more than 0.8% in the central Pacific. No anisotropy determinations have been made for the Atlantic Ocean basins. The azimuthal difference between the two paths in Figure 1 is only 20°, and an anisotropy of at least 8% is required to explain the interstation variation.

Surface waves travel a least time rather than a least distance path, and in the presence of lateral velocity changes the true path may deviate from a great circle. The clean appearance of the seismograms in Figure 2, especially at SDB, argues against significant multipath transmission. Station timing errors were checked by measuring the P arrival times on the short period vertical seismograms. Residuals are smaller than 1 s using the travel time tables of Herrin [1968].

The uncertainties given in Table 2 are the root-mean-square sum of the standard errors from the group velocity measurement, the epicenter mislocation error, the origin time error, and the source finiteness error. This is the best estimate available and probably overestimates the true uncertainty.

The differences observed between the on-ridge and off-ridge dispersion are real and cannot be eliminated even by consideration of cumulative small errors. This implies that there is unusual velocity structure associated with the Walvis Ridge rather than an anomaly of more regional extent.

Inversion

In Figure 3 the group velocities for both South Atlantic paths are compared to the 20 to 50 m.y. curve from Forsyth [1973] for the Pacific. For both measurements the group velocity at periods out to 30–40 s is significantly lower, indicating a deficiency of high velocity material in the upper layers. Marked differences between the shapes of the two South Atlantic curves and between them and the Pacific curve are seen and cannot be eliminated by the errors discussed in the last section. Since dispersion curve shape reflects the velocity distribution with depth more than its actual magnitude, some variation on the usual monotonic decrease in shear velocity with depth down to the low velocity zone is expected along both paths. The difference is more marked for the on-ridge (SDB) path. Long period discrepancies are apparent but involve only a few data points at periods where spectral resolution is not high and should not be emphasized.

Most velocity models derived from surface wave dispersion are fit to the data without indicating which features of the model are actually required by the data. Modern inverse theory gives a way to determine both the necessary model parameters and the resolution of the individual layers. The details of this technique can be found in the literature [Jackson, 1972; Wiggins, 1972] and will only be outlined here. A starting model is proposed, used to compute the partial derivatives of the data with respect to the unknowns, and compared to the data. First order corrections to the model are derived and applied to it, and the process is repeated iteratively until changes to the model are small. The layer structure remains unchanged during the inversion so that the result is influenced by the choice of a starting model. Owing to nonlinearity, the trade-off between shallow and deep structural changes, and the lack of other data to constrain the inversion, the smallest difference from a standard earth model, used as a starting model, was searched for by trial and error modification of the layer thicknesses. The partial derivatives are recomputed for each iteration, significantly increasing the parameter range for convergence with a given starting model.

Rayleigh waves are sensitive to a combination of shear and compressional wave velocity, and density. Most inversions have focused on shear velocity since its effect is large at all depths, but compressional velocity and density may exert a significant influence near the surface. Figure 4 shows the partial derivatives of group velocity with respect to all three parameters for the final on-ridge model. It is clear that compressional velocity is not a major factor except in the water and upper crustal layers to depths of 5 km and can safely be neglected unless details of the crustal structure are desired and can be resolved. Density can affect the results into the upper mantle and in the low-velocity zone. Since no good independent way to estimate mantle density exists, the data were inverted for shear velocity alone. The effect of density changes in the final model were then evaluated by perturbing the layer densities at different depths. It should be noted that the shear velocity and density partial derivatives have different signs near the surface at all periods; hence a decrease in near-surface density implies an increase in shear velocity, and vice versa.

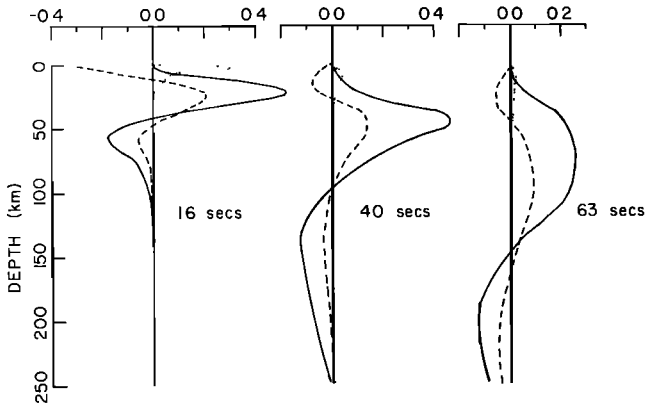

Fig. 4. Partial derivatives of group velocity at 16-, 40- and 63-s periods with respect to compressional velocity (dotted line), shear velocity (solid line), and density (dashed line) for the final ridge model.

The starting model was similar to that of Forsyth [1973, 1975] and to simple oceanic models from Knopoff [1972]. It consists of a water layer, a single crustal layer, a high-velocity upper mantle lid, a low-velocity channel, a subchannel layer, and a half space. The water depth was measured on the bathymetric charts of E. Uchupi and H. Hays [unpublished data, 1978], and an average for the great circle path was taken. Sediment cover on the Walvis Ridge is patchy, reaching 1 km only in isolated places [Dingle and Simpson, 1976] and is no more than 400 m thick in the Cape Basin [Ewing et al., 1966], so no sediment layer was included. The crustal velocity was an average for layer 3 from Christensen and Salisbury [1975]. The upper mantle velocities and densities are from Forsyth (1973). The compressional velocity was fixed at 8.0 km/s except in the low velocity zone, where 7.8 km/s was used. Mantle density was set at 3.4 and crustal density at 3.0 g/cm^3. Typically, three or four iterations sufficed for convergence of the inversion. The final models were then checked and found to be insensitive to the starting shear velocities.

Results

Figure 5 shows the best models for both the on-ridge (SDB) and off-ridge (WIN) paths compared to the velocity structure for 20 to 50 m.y. lithosphere in the east Pacific [Forsyth, 1973]. Table 3 lists the final model parameters and the standard deviations for the shear velocities in each layer. Since the paths in this study are orthogonal to the isochrons, the dispersion should reflect a velocity structure that is an average for lithosphere of zero age to the early opening of the South Atlantic at about 130 Ma (Ma = m.y. B.P.). The velocity structure of the oceanic upper mantle evolves rapidly for the first 50 m.y. Changes in the velocity structure for older lithosphere are small, amounting to no more than 0.1 km/s [Forsyth, 1977], and the 20 to 50-m.y. structure is a representative average for normal oceanic lithosphere. Studies in the Atlantic indicate somewhat higher upper mantle shear velocity than in the Pacific structure [Weidner, 1973]. Figures 6 and 7 are the residuals and resolving kernels for the respective models. The fit to the data is good at all except the shortest periods, where water depth variations, sediment thickness and velocity variations, and crustal inhomogeneity along the path will cause significant lateral refraction and increase the scatter in the data. In the off-ridge model the longest and shortest period data seriously degraded the results and were not used in the final inversion.

The resolving kernels of Figure 7 can be thought of as windows through which the velocity structure is viewed. If the individual layers are perfectly resolved, then only the velocity of one layer will be seen for each kernel. The widths of the kernels determine the depth resolution at each layer. A trade-off between layer thickness and shear velocity is possible, and well-resolved layers can mean poorly known velocities. Table 3 lists the standard deviations of the layer shear velocities. It is clear that the good depth resolution implied by Figure 7 is matched by good resolution of the velocities within each layer. The resolving kernels are compact, with little trade-off possible between different parts of the model. Attempts to increase the number of layers resulted in solutions that were oscillatory and in noncompact resolving kernels, probably owing to the lack of phase velocity measurements and errors in the data. Features of both solutions include well resolved upper mantle lids and only limited interaction of near surface layers

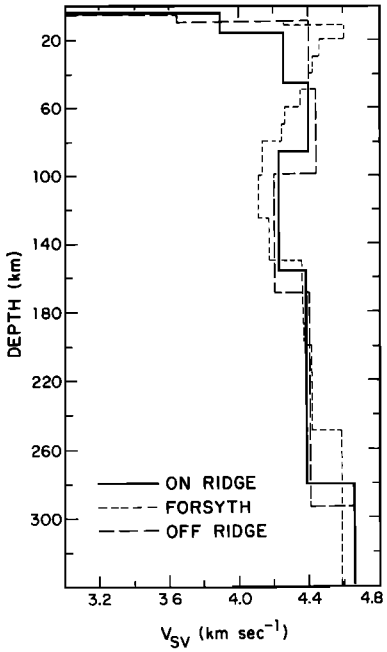

Fig. 5. Models of the shear velocity structure resulting from the inversion of the two dispersion curves compared to the 20 to 50 m.y. structure of Forsyth [1973]. The solid line is for the on-ridge (SDB) path, the long-dashed line is for the off-ridge (WIN) path, and the short-dashed line is for Forsyth's result.

TABLE 3. Final Model Parameters

Layer	Thickness	V_p	V_s	$\pm\sigma$	Density
			On-Ridge (SDB)		
1	3.5	1.52	0.00	0.000	1.03
2	12.5	7.00	3.90	0.076	3.00
3	30.0	8.00	4.26	0.023	3.40
4	40.0	8.00	4.40	0.023	3.40
5	70.0	7.80	4.21	0.039	3.40
6	125.0	7.80	4.37	0.026	3.40
7	Half space	8.00	4.65	0.000	3.40
			Off-Ridge (WIN)		
1	4.5	1.52	0.00	0.000	1.03
2	5.0	6.70	3.65	0.000	2.90
3	40.0	8.00	4.40	0.010	3.40
4	50.0	8.00	4.44	0.017	3.40
5	70.0	7.80	4.20	0.048	3.40
6	125.0	7.80	4.41	0.012	3.40
7	Half space	8.00	4.65	0.000	3.40

with the low-velocity zone. Resolution is poor below 150 km, reflecting the lack of data beyond 90 s in period.

While surface wave dispersion data cannot locate sharp discontinuities in velocity very precisely due to inherent smoothing of the structure, some estimate of their position can be obtained by studying the effect of layer thickness on layer velocity. The choice of mantle lid thickness is bounded by the inability to resolve channel from subchannel for too thin a layer and unreasonably low subchannel velocities as the thickness increases. Sudden changes in the layer velocities indicate the approximate locations of major boundaries, especially the lid-channel transition. The resulting mantle lid is 70 km thick for the on-ridge model and 90 km thick for the off-ridge model, with uncertainties of 10-20 km. This gives a total lithospheric thickness, assuming the low-velocity zone to mark the lithosphere-asthenosphere boundary, of

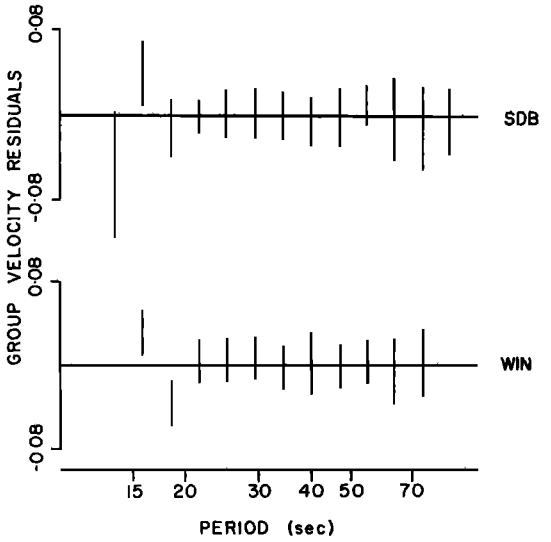

Fig 6. Residuals for the (top) on-ridge and (bottom) off-ridge models.

80-100 km for both cases. Given the possible resolution in the upper 100 km no significant thinning of the lithosphere is seen under the Walvis Ridge. No major differences from normal oceanic lithosphere exist below 50 km for either path.

The on-ridge structure requires both crustal thickening to 12.5 ± 3 km and low velocity (V_s = 4.26 km/s) upper mantle. The uncertainty in crustal thickness was measured by varying the crustal thickness and requiring the velocity to be within the layer 3 range determined by Christensen and Salisbury [1975]. Splitting the crust into layers 2 and 3 results in slight crustal thinning, but the data cannot resolve such detail. Lowering the integrated crustal velocity raises the mantle velocity by 0.06 km/s, meaning that a finer crustal structure would increase it. Changes in mantle lid velocity do not significantly affect the crustal velocities. The low mantle lid velocity is significant when compared to an average of 4.50 km/s for the Pacific model. Since half of the path traverses lithosphere older than 50 m.y., the normal mantle shear velocity should be at least this high.

No crustal thickening is seen for the off-ridge path. Attempts to increase the thickness of the crust result in interaction with the deep layers and unreasonably high velocities. The upper mantle lid velocity is 4.40 km/s, which is intermediate between the off-ridge and normal results.

The partial derivatives of Figure 4 indicate that lowered density in the near surface layers can increase the apparent shear velocity in nearby layers. If the top 30 km of the on-ridge mantle lid has a density of 3.2 instead of 3.4, then the upper lid shear velocity rises to 4.30 km/s and the lower lid velocity falls to 4.33 km/s. Crustal density decreases do not appreciably influence mantle velocities but do change the crustal velocities and reduce the apparent crustal thickness. It is unlikely that the mantle density is higher than 3.4; hence the structure of Figure 5

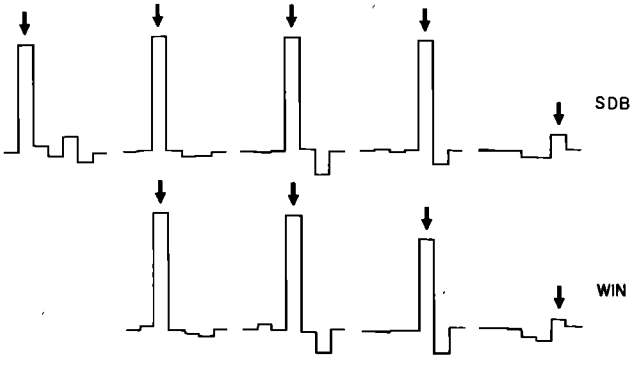

Fig. 7. Resolving kernels for the (top) on-ridge and (bottom) off-ridge models for, from left to right, the second through sixth layers of Table 3. The arrows point to the layer on which the parameter is centered. See text for discussion.

should be regarded as a lower limit rather than an average. Rayleigh wave dispersion data alone cannot differentiate the effects of low density and low velocity.

Discussion

The models presented in the last section are averages for the great circle paths of Figure 1. Lateral differences can be resolved only if many different size samples of the different regions can be measured over multiple paths. Such a procedure has been used in 'pure path' studies [Dziewonski, 1971; Forsyth, 1973, 1975] but is not applicable to the limited data in this work. Gravity data suggest different crustal thicknesses and isostatic compensation mechanisms for the eastern and western parts of the Walvis Ridge. The former is not incompatible with the surface wave determined structure, since the 12.5 km crust inferred in this work is intermediate between a 5 to 8 km thickness for the seamount province and a 15 to 30 km thickness for the block ridge province given by Detrick and Watts [1979]. The inability to fit a thick crust to the WIN data also suggests that differences along the strike of the ridge are present.

The off-ridge path samples the western seamount-guyot region as well as a section of the Cape Basin (Figure 1). If the dispersion curve for the on-ridge path is taken to represent the western Walvis Ridge, then the off-ridge path can be separated into two regions by subtraction of the group slownesses for the two paths after choosing appropriate regional boundaries. The result for the Cape Basin is not significantly different from the 100 to 135 m.y. curve of Forsyth [1977] except at short periods where crustal differences control the dispersion. Such a crude calculation is heavily influenced by the assumed regionalization and is not statistically rigorous. Nevertheless, it suggests that the anomalous mantle region may not extend beyond a few hundred kilometers from the ridge axis.

Poisson's ratio (σ) is an elastic parameter that can be calculated if both compressional and shear velocity are known. Most peridotitic mantle materials are characterized by σ values of 0.27-0.28 [Ringwood, 1975]. If the mantle shear velocity is in the range of 4.25-4.35 km/s and σ is 0.28 the compressional velocity must be 7.7-7.9 km/s. This is slightly lower than that reported from seismic refraction on the Nazca Ridge [Cutler, 1977]. It must be emphasized that seismic refraction measures the velocity beneath an interface, while surface wave dispersion yields an average velocity over a depth interval. Direct comparisons of them are difficult.

Low shear velocity in mantle rock can be caused by elevated temperature and partial melting. The temperature partial derivatives for many mantle materials have been measured in the laboratory. Using a value given by Chung [1976] for an artificial peridotite, a normal mantle velocity of 4.60 km/s, and a decrease of 0.30 km/s for the Walvis Ridge yields a temperature anomaly of 800°C. Superimposed on a normal sub-Moho temperature of 300°C, this gives an upper mantle at temperatures of at least 1100°C at a depth near 15 km. The solidus temperature of a pyrolite mantle, while strongly influenced by water content, is not over 1200°C [Ringwood, 1975], and incipient partial melting at shallow depths will result. A very small partial melt fraction, no more than a few percent, can easily produce the velocity anomaly that is seen [Anderson and Sammis, 1970].

Neither high temperature nor partial melting is consistent with other geophysical evidence. Hot material at shallow depths must produce surface heat flow effects. If the upper mantle temperature is 1000°C at a depth of 15 km and the thermal conductivity is 0.006 cal $^{\circ}C^{-1}$ cm^{-1} s^{-1}, the surface heat flow is at least 4 HFU (1 HFU = 1 μcal cm^{-2} s^{-1}). The observed heat flow is only 2 HFU, or 0.7 HFU above that in the surrounding ocean basins, probably a result of a larger reservoir of radioactive material [Lee and Von Herzen, 1977]. High temperature in the mantle will lead to thermal expansion and density changes which will produce large regional elevation anomalies. Uplift of several kilometers must result from the effective lithospheric thinning due to the high temperature, as may occur under mid-ocean island swells [Detrick and Crough, 1978; Crough, 1978]. No noticeable long wavelength bathymetric features are apparent on either bathymetric charts or profiles crossing the Walvis Ridge. For these reasons an alternate hypothesis must be sought.

Compositional zoning in the mantle, especially that associated with supposed mantle plumes, has received increasing geochemical support [Schilling, 1973, 1975]. Trace element data, particularly strontium and lead isotopic data, indicate marked differences of the mantle sources for Walvis Ridge volcanics from those in other oceanic provinces [Gast et al., 1964; Oversby and Gast, 1970]. It is likely that the low mantle velocity under the Walvis Ridge is due to unusual mantle composition associated with the surface geochemical anomalies.

Quantitative correlation of the geophysical and geochemical evidence requires more complete petrological and laboratory data.

Conclusions

From the Rayleigh wave dispersion study of the Walvis Ridge the following conclusions can be drawn:

1. The Walvis Ridge exhibits an average crustal thickness that is 1.5-2 times the oceanic norm. This is consistent with the limited seismic refraction data for aseismic ridges and a gravity study on the Walvis Ridge by Detrick and Watts [1979].

2. The top 30 km of upper mantle under the Walvis Ridge is composed of low shear velocity material (V_S = 4.25-4.35 km/s). Even if the mantle density is as low as 3.2 g/cm^3 to depths of 40-50 km, the shear velocity in the mantle is far below the normal value for oceanic lithosphere of moderate age.

3. The low-velocity cannot be explained by partial melting or high temperature at the base of the crust, since the observed heat flow and regional elevation is not radically different from that in the surrounding ocean basins. The low shear velocity may be due to compositional zoning of the mantle.

Acknowledgements. S. T. Crough encouraged me to pursue this work. C. R. Denham and R. P. Von Herzen provided helpful discussions. J. D. Phillips and D. W. McCowan provided access to William Rodi's inversion program and the computer facilities at Lincoln Laboratory, which is supported by the Defense Advanced Research Projects Agency. Sandy Tonge typed the manuscript. This work was supported by a National Science Foundation Graduate Fellowship and the WHOI Education Office. This is Woods Hole Oceanographic Institution Contribution 4298.

References

Anderson, D., and C. Sammis, Partial melting in the upper mantle, Phys. Earth Planet. Interiors, 3, 41-50, 1970

Bott, M. H. P., C. W. A. Browitt, and A. P. Stacey, The deep structure of the Iceland-Faeroe Ridge, Mar. Geophys. Res., 1, 328-357, 1971.

Brune, J. N., Correction of initial phase measurements for the southeast Alaska earthquake of July 10, 1958, and for certain nuclear explosions, J. Geophys. Res., 67, 3643-3644, 1962.

Christensen, N. I., and M. H. Salisbury, Structure and constitution of the lower oceanic crust, Rev. Geophys. Sp. Phys., 13, 57-86, 1975.

Chung, D. H., On the composition of the oceanic lithosphere, J. Geophys. Res., 81, 4129-4134, 1976.

Crough, S. T., Thermal origin of mid-plate hot-spot swells, Geophys. J. Roy. Astron. Soc., 55, 451-469, 1978.

Cutler, S.T., Geophysical investigation of the Nazca Ridge, M.S. thesis, Univ. of Hawaii, Honolulu, 1977.

Der, Z., R. Masse, and M. Landisman, Effects of observational errors on the resolution of surface waves at intermediate distances, J. Geophys. Res., 75, 3399-3409, 1970.

Detrick, R. S., and S. T. Crough, Island subsidence, hot spots, and lithospheric thinning, J. Geophys. Res., 83, 1236-1244, 1978.

Detrick, R. S., and A. B. Watts, An analysis of isostasy in the world's oceans: part 3 - aseismic ridges, J. Geophys. Res., 84, 3637-3653, 1979.

Detrick, R. S., J. G. Sclater, and J. Thiede, The subsidence of aseismic ridges, Earth Planet. Sci. Lett., 34, 185-196, 1977.

Dingle, R. V., and E. S. W. Simpson, The Walvis Ridge: a review, in Geodynamics: Progress and Prospects, edited by C. L. Drake, pp. 160-176, AGU, Washington, D.C., 1976.

Dziewonski, A., Upper mantle models from 'pure path' dispersion data, J. Geophys. Res., 76, 2587-2601, 1971.

Dziewonski, A., S. Block, and M. Landisman, A technique for the analysis of transient seismic signals, Bull. Seism. Soc. Am., 59, 427-444, 1969.

Ewing, M., X. LePichon, and J. Ewing, Crustal structure of the mid ocean ridges, 4, Sediment distribution in the South Atlantic Ocean and the Cenozoic history of the Mid-Atlantic Ridge, J. Geophys. Res., 71, 1611-1636, 1966.

Forsyth, D. W., Anisotropy and the structural evolution of the oceanic upper mantle, Ph.D. thesis, 255 pp., Mass. Inst. of Technol. and Woods Hole Oceanogr. Inst., Cambridge, 1973.

Forsyth, D. W., Anisotropy and the structural evolution of the oceanic upper mantle, Geophys. J. Roy. Astron. Soc., 43, 103-162, 1975.

Forsyth, D. W., The evolution of the upper mantle beneath mid-ocean ridges, Tectonophysics, 38, 89-118, 1977.

Forsyth, D. W., and F. Press, Geophysical tests of petrological models of the spreading lithosphere, J. Geophys. Res., 76, 7963-7979, 1971.

Gast, P. W., G. R. Tilton, and C. Hedge, Isotopic composition of lead and strontium from Ascension and Gough Islands, Science, 145, 1181-1185, 1964.

Goslin, J., and J.-C. Sibuet, Geophysical study of the easternmost Walvis Ridge, South Atlantic: Deep structure, Geol. Soc. Amer. Bull., 86, 1713-1724, 1975.

Hagiwara, T., A note on the theory of the electromagnetic seismograph, Bull. Earthquake Res. Inst. Tokyo Univ., 36, 139-164, 1958.

Hanks, T. C., and W. Thatcher, A graphical representation of seismic source parameters, J. Geophys. Res., 77, 4393-4405, 1972.

Herrin, E. (chairman), 1968 seismological tables for P phases, Bull. Seism. Soc. Amer., 58, 1193, 1968.

Jackson, D. D., Interpretation of inaccurate, insufficient and inconsistent data, Geophys. J. Roy. Astron. Soc., 28, 97-109, 1972.

Kanamori, H., The Alaska earthquake of 1964: Radiation of long-period surface waves and

source mechanism, J. Geophys. Res., 75, 5029-5040, 1970.
Knopoff, L., Observation and inversion of surface wave dispersion, Tectonophysics, 13, 497-519, 1972.
Kogan, M. G., The gravity field of oceanic block ridges, Izv. Acad. Sci. USSR Phys., Solid Earth, 12, 710-717, 1976.
Lee, T. -C., and R. P. Von Herzen, A composite trans-Atlantic heat flow profile between 20°S and 35°S, Earth Planet. Sci. Lett., 35, 123-133, 1977.
Mitchell, B. J., and M. Landisman, Electromagnetic seismograph constants by least squares inversion, Bull. Seismol. Soc. Amer., 59, 1335-1348, 1969.
Morgan, J., Convection plumes in the lower mantle, Nature, 230, 42.
Morgan, J., Plate motions and deep mantle convection, Geol. Soc. Am. Mem., 132, 7, 1972.
Oversby, V., and P. M. Gast, Isotopic composition of lead from oceanic islands, J. Geophys. Res., 75, 2097-2114, 1970.
Ringwood, A. E., Composition and Petrology of the Earth's Mantle, 618 pp., McGraw-Hill, New York, 1975.
Schilling, J. -G., Iceland mantle plume, Nature, 246, 104, 1973.
Schilling, J. -G., Azores mantle blob: rare earth evidence, Earth Planet. Sci. Lett., 25, 103-115, 1975.
Stewart, I. C. F., and C. E. Keen, Anomalous upper mantle structure beneath the Cretaceous Fogo seamounts indicated by P-wave reflection delays, Nature, 274, 788-791, 1978.
Thomas, P. D., Geodesic arc length on the reference ellipsoid to second order terms in the flattening, J. Geophys. Res., 70, 3331-3340, 1965.
Weidner, D. J., Rayleigh-wave phase velocities in the Atlantic Ocean, Geophys. J. Roy. Astron. Soc., 36, 105-139, 1973.
Weigel, W., P. Goldflam, and K. Hinz, The crustal structure of Concepcion Bank, Mar. Geophys. Res., 3, 381-392, 1978.
Wiggins, R., The general linear inverse problem: implications of surface waves and free oscillations for earth structure, Rev. Geophys. Space Phys., 10, 251-285, 1972.
Wilson, J. T., Evidence from islands on the spreading of ocean floors, Nature, 197, 536-538, 1963.
Yu, G. -K., and B. J. Mitchell, Regionalized shear velocity models of the Pacific upper mantle from observed Love and Rayleigh wave dispersion, Geophys. J. Roy. Astron. Soc., 57, 311-341, 1979.

(Received February 15, 1979;
revised June 25, 1979;
accepted July 10, 1979.)